DOI: 10.1002/chem.200902546

Quantifying the Effect of Surface Ligands on Dendron–DNA Interactions: Insights into Multivalency through a Combined Experimental and Theoretical Approach

Simon P. Jones,[a] Giovanni M. Pavan,*[b, c] Andrea Danani,[b] Sabrina Pricl,[c] and David K. Smith*[a]

Abstract: We report the synthesis, DNA binding ability and preliminary gene delivery profiles of dendrons with different amine surface groups, 1,3-diaminopropane (DAP), *N*,*N*-di-(3-aminopropyl)-*N*-(methyl)amine (DAPMA) and spermine (SPM). By using a combination of ethidium bromide displacement, gel electrophoresis and transfection assays, it is shown that the dendrons with SPM groups are the most effective DNA binders, while the DAPMA-functionalised dendrons were the most effective systems for gene delivery (although the gene delivery profiles were still modest). In order to provide deeper insight into the experimental data, we performed a molecular dynamics simulation of the interactions between the dendrons and DNA. The results of these simulations demonstrated that, in general terms, the enthalpic contribution to binding was roughly proportional to the dendron surface charge, but that dendrons with DAP (and DAPMA) surface amines had significant entropic costs of binding to DNA. In the case of DAP, this is a consequence of the fact that the entire dendron structure has to be organised in order for each individual monoamine charge to make effective contact with DNA. For SPM, however, each surface ligand is already a multivalent triamine, therefore, each individual charge has a much lower entropic cost of binding. For DAPMA, we observed that strong binding of the hindered tertiary amine to the DNA double helix led to ligand back-folding and significant geometric distortion of DNA. Although this weakens the overall binding, we suggest that this distortion might be an explanation for the experimentally observed enhanced gene delivery, in which DNA compaction is an important step. Overall, this paper demonstrates how structure–activity relationships can be developed for multivalent dendritic ligands and provides insights into the thermodynamics of multivalent interactions.

Keywords: dendrimers · DNA · gene technology · molecular dynamics · thermodynamics

Introduction

Multivalent binding of biological targets is a key principle in enhancing binding strength and hence developing systems with potential biomedical applications.[1] By employing multivalent ligand arrays, synthetic systems are able to enhance their binding to targets with more than one binding site. Experimental studies and mathematical models have demonstrated that once the first ligand in a multivalent array has bound to the target, the binding of a second ligand will be a cooperative, entropically less disfavoured process, with a local concentration effect also enhancing binding.[2] Dendrimers and dendrons are well-defined nanoscale branched polymers that have repetitive structures and multiple surface groups, and as such they are of great interest for their participation in biologically-relevant multivalent recognition processes.[3] There has been considerable interest in the ability

[a] Dr. S. P. Jones, Prof. D. K. Smith
Department of Chemistry, University of York
Heslington, York, YO10 5DD (UK)
Fax: (+44) 1904 432516
E-mail: dks3@york.ac.uk

[b] G. M. Pavan, Prof. A. Danani
University for Applied Sciences of Southern Switzerland (SUPSI)
Institute of Computer Integrated Manufacturing
for Sustainable Innovation
Centro Galleria 2, 6928 Manno (Switzerland)
Fax: (+41) 58 666 6620
E-mail: giovanni.pavan@supsi.ch

[c] G. M. Pavan, Prof. S. Pricl
Molecular Simulations Engineering (MOSE) Laboratory
Department of Chemical Engineering (DICAMP)
University of Trieste
Piazzale Europa 1, 34127 Trieste (Italy)

Supporting information for this article is available on the WWW under http://dx.doi.org/10.1002/chem.200902546.

of dendritic molecules to interact with nucleic acid targets, such as DNA and RNA.[4] Nucleic acids have multiple potential sites with which ligands can interact. In general terms, cationic ligands interact with polyanionic DNA/RNA, and the organisation of multiple charge–charge interactions can give rise to high-affinity nucleic acid binding.[5] The first studies of interactions between cationic dendrimers and DNA were performed by the groups of Tomalia and Szoka, who employed high generation spherical poly(amidoamine) (PAMAM) dendrimers.[6] These polycationic, multivalent dendrimers show high affinity for DNA and can achieve effective gene delivery into cells.[7] Computer modelling of the interactions between these dendrimers and single strand DNA suggested that at high dendritic generations of growth, single strand DNA could wrap itself around the large surface of the dendrimer.[8] Since these studies, a wide range of polycationic multivalent dendrimers and dendrons have been employed in DNA binding and gene delivery, including systems based on dendritic poly(L-lysine),[9] poly(propyleneimine),[10] and other more specialised dendritic frameworks.[11] In general, the affinity of dendritic molecules towards DNA binding increases as they get larger (increasing dendritic generation). This reflects the fact that the primary interactions between cationic dendrimers and DNA are electrostatic in nature. Gene delivery profiles also usually improve at higher dendritic generation, for example, PAMAM dendrimers exhibit optimal gene delivery at about the fifth generation of growth (G5).[12] In addition to using simple monoamine surface groups on dendritic structures, there has been some interest in how the precise structure of the cationic surface groups modifies DNA binding and gene delivery. For example, dendritic surfaces have frequently been functionalised with cationic arginine (guanidinium) surface groups; this is a way of significantly enhancing gene delivery.[13]

We have recently developed a biomimetic approach to multivalent DNA binding dendrons and synthesised dendritic arrays of spermine ligands.[14] Spermine is a naturally occurring tetra-amine that is used in nature for DNA binding and present in millimolar amounts in eukaryotic cells.[15] Spermine plays a key role in the compaction of DNA, and there has been considerable interest in the mode of DNA binding, and mechanisms through which oligoamines of this type can modify the conformation of DNA, for example, by inducing bending and aggregation.[16] Although a tetra-amine, the interaction between an individual spemine ligand and DNA is still relatively weak especially in the competitive high salt environment of biological systems.[17] We have reported that dendritic arrays of spermine units can give rise to much enhanced ultrahigh affinity DNA binding.[14] We employed an ethidium bromide (EthBr) displacement assay to gain a comparative quantitative estimate of the binding strengths, and discovered that the second generation system (G2-SPM, Figure 1) with nine surface spermine ligands, displaced 50% of EthBr from its complex with DNA (ca. 1 μM) at concentrations as low as 30 nM. This was a significantly lower concentration than that required for monovalent spermine (high micromolar concentrations). Furthermore, the binding of G2-SPM to DNA was independent of salt concentration, and in a recent modelling study we proposed that for the second generation system under high salt conditions, some of the spermine surface groups effectively "sacrificed" their interaction with DNA and acted to screen/optimise the remaining spermine ligands that then bound to the DNA more tightly than would have been expected.[18] In this way, the dendrimer exhibited a new type of multivalency effect. We have experimentally explored the effects of dendron structural variation on DNA binding, in order to develop structure–activity relationships. We have grafted the dendritic spermine array onto proteins and demonstrated that the synthetic nanoscale biohybrids exhibit high DNA affinity,[19]

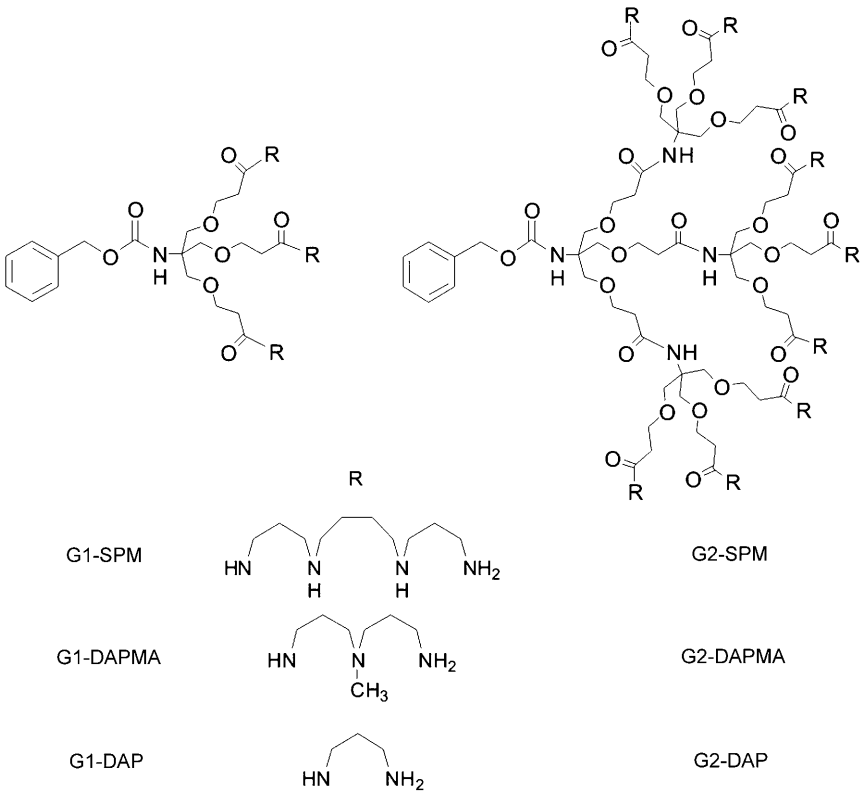

Figure 1. Chemical structures of the dendrons investigated in this study.

modified the structures of the dendrons such that cellular gene delivery can be achieved,[20] and both ourselves and Kostiainen et al. have developed degradable systems, in which the multiple spermine ligands are cleaved from the surface of the dendron, "switching off" the high-affinity binding.[21] However, we were also interested in the precise role played by the spermine ligands in binding to the DNA. In order to probe this in more detail, we decided to synthesise a family of dendrons with different surface groups (Figure 1). The comparison between these systems and their ability to bind and deliver DNA is the subject of this study. We have employed a combined experimental and theoretical (molecular dynamics modelling) approach in order to gain a unique insight into the behaviour of these dendrons and the role played by the surface groups in controlling their multivalent interactions with DNA.

Results and Discussion

Experimental Study

Synthesis: Compounds G1-SPM and G2-SPM were synthesised using our previously reported methods.[14] We then selected commercially available amines that could be readily modified using simple syntheses—diaminopropane (DAP) and *N*,*N*-di-(3-aminopropyl)-*N*-(methyl)amine (DAPMA)—for attachment to the same Newkome-type dendron scaffold.[22] It is worth noting that each spermine (SPM) ligand has three protonatable amines once it is attached to the dendritic scaffold through an amide linkage, while each DAPMA group has two, and each DAP group only has one. Both DAP and DAPMA could be readily monoprotected with *tert*-butoxycarbonyl (Boc) groups on one of the two terminal primary amines (Scheme 1).[23] This enabled the incorporation of these protected amines onto the periphery of the previously reported first and second generation dendritic scaffolds (G1 and G2) by simple amide coupling methodologies. The yields for surface functionalisation of the first generation dendron were acceptable (about 30%) with G1-DAP(Boc) and G1-DAPMA(Boc) being obtained in high purity after column chromatography. The yield for ninefold functionalisation of the second generation dendron with DAPMA(Boc) to give G2-DAPMA(Boc) was very low (ca. 5%) but this was sufficient to provide enough material for biological studies, and we therefore did not pursue the optimisation of this procedure further at this point. On the other hand, pure products could not be obtained when using DAP(Boc) in an attempt to yield G2-DAP(Boc). We suggest that this latter reaction might have failed due to the greater steric hindrance of the reactive amine in DAP(Boc) caused by the proximate Boc protecting group when compared with the more distant Boc protecting group in DAPMA(Boc). Consideration of the modelling studies (see below) meant that we did not pursue the synthesis of G2-DAP(Boc) any further at this point. Deprotection of the peripheral Boc groups by using hydrogen chloride in methanol finally yielded the target amine-surfaced dendrons (G1-DAP, G1-DAPMA and G2-DAPMA) as their hydrochloride salts in excellent yield.

Ethidium bromide displacement: In order to gain a comparative quantification of the DNA binding abilities of these dendrons, we employed an ethidium bromide (EthBr) displacement fluorescence assay, which is commonly used to investigate the binding of polyammonium cations to calf thymus DNA.[14,21,24] When EthBr is displaced from its complex with DNA, the fluorescence intensity decreases, allowing quantification of the amount of dendron required to effectively bind DNA. This is most usually expressed as the "charge excess" of cationic dendron relative to anionic DNA required for 50% EthBr displacement (CE_{50}, Table 1). The concentration of dendron required for effective DNA binding can also be calculated (C_{50}, Table 1). It should be noted that EthBr displacement is a competitive binding assay, and therefore only really appropriate for comparing ligands with similar DNA binding modes: in this case, all of the dendrons have polyamine surfaces, and we reasoned that comparison was valid.

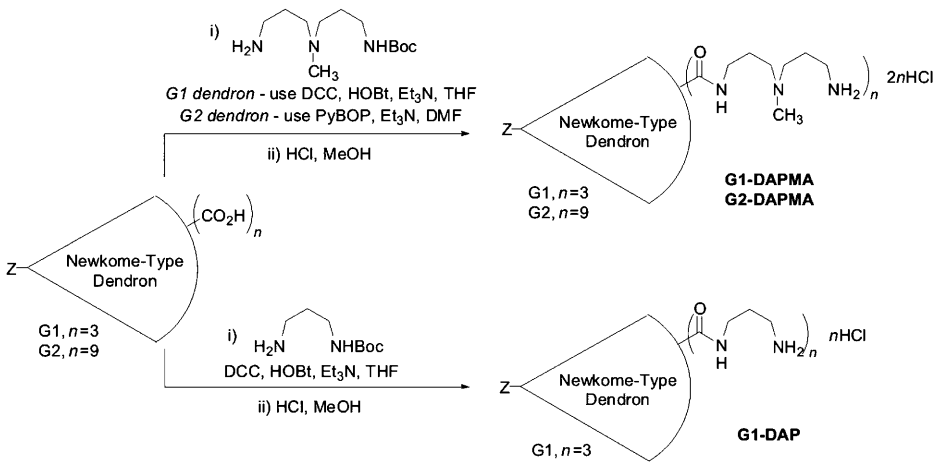

Scheme 1. Synthesis of DNA binding dendrons G1-DAPMA, G2-DAPMA and G1-DAP.

The data in Table 1 indicate that for each type of dendron, the G2 systems are significantly better DNA binders than their G1 analogues—a clear multivalency effect. Dendrons G1-SPM and G2-SPM are the most effective DNA binders in terms of the CE_{50} parameter, which reflects the relative ability of the cationic charges to bind anionic DNA. Consideration of

Table 1. DNA binding data extracted from ethidium bromide (EthBr) displacement assays. Assays were performed by using EthBr (2.54 μM) and calf thymus DNA (1.00 μM double stranded concentration; the concentration of each negatively charged phosphate is therefore 2.00 μM).

Dendron	CE_{50} value[a]	C_{50} value[b] [μM]	$[Amine]_{50}$[c] [μM]
G1-DAP	550[d]	367	1100
G1-DAPMA	32	10.7	32
G2-DAPMA	5.1	0.567	5.1
G1-SPM	2.7	0.600	1.8
G2-SPM	0.76	0.056	0.50

[a] CE_{50} represents the charge excess (N:P ratio) required to decrease EthBr fluorescence by 50%. [b] C_{50} represents the concentration of dendron required to displace 50% of EthBr. $C_{50} = CE_{50} \times 2.00$ μM/No. of protonatable amines in the dendron. [c] $[Amine]_{50}$ represents the effective (normalised) concentration of amine surface ligand required to displace 50% of EthBr; $[amine]_{50} = C_{50} \times$ No. of surface ligands on dendron. [d] This value was estimated by linear extrapolation of the data points.

the $[amine]_{50}$ parameter again shows that spermine is the optimal surface ligand for DNA binding, outperforming DAPMA by an order of magnitude and DAP by three orders of magnitude when attached to the same dendron support. In concentration terms, the performance of G2-DAPMA with nine surface ligands is similar to that of G1-SPM, which only has three spermine ligands, even though the former has 18 surface positive charges and the latter only has nine. This clearly demonstrates that G1-SPM employs its ligands for DNA binding more effectively than G2-DAPMA and shows that it is not *just* their higher charge that gives spermine ligands their DNA binding advantage. It is worth noting that spermine is optimised in nature for minor groove DNA binding, whereas the synthetic amines (DAP and DAPMA) are not.

Gel electrophoresis: Gel electrophoresis was also used to provide complementary insight into DNA binding (Figure 2); the DNA used was a pGL3 plasmid instead of calf thymus DNA in order to obtain good electropherograms. We discontinued experimental work with G1-DAP as the DNA binding was too weak to quantify in a meaningful way, and focused on the DAPMA-functionalised dendrons, which had shown a degree of effective DNA binding (Figure 2). Dendron G1-DAPMA showed relatively weak DNA binding and condensation by electrophoresis, as would be expected from the EthBr assay. Dendron G1-DAPMA showed some retardation of DNA migration from 0.6–1.5 (*w*/*w*) ratio (0.59 to 1.76 nmoles) and complete retardation at higher ratios. On the other hand, G2-DAPMA retarded DNA migration at 0.7:1 (*w*/*w*; 0.23 nmoles); this is in agreement with the hypothesis that multivalent G2-DAPMA is a more effective DNA binder than G1-DAPMA. The DNA binding achieved by G2-DAPMA is less effective than that previously observed by using G2-SPM (retardation at 0.5:1, *w*/*w*, corresponding to 0.12 nmoles).[20a] This difference is somewhat smaller than what might have been anticipated from the EthBr assay. It should be noted, however, that the

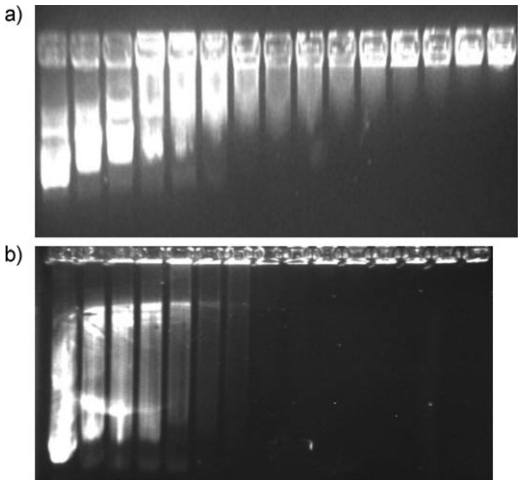

Figure 2. Gel electrophoresis of DAPMA dendrons: a) Z-G1-DAPMA, and b) Z-G2-DAPMA (polyamine:DNA, *w*/*w*); lane 1: 0:1; lane 2: 0.1:1; lane 3: 0.2:1; lane 4: 0.3:1; lane 5: 0.4:1; lane 6: 0.5:1; lane 7: 0.6:1; lane 8: 0.7:1; lane 9: 0.8:1; lane 10: 0.9:1; lane 11: 1:1; lane 12: 1.5:1; lane 13: 2:1; lane 14: 2.5:1; lane 15: 3:1.

EthBr displacement assay is a competition experiment, and is only at its most effective when comparing directly equivalent ligands. It should also be noted that gel electrophoresis depends on effective DNA compaction, and this can differ between the different classes of surface ligand (see modelling study later for further discussion).

Gene transfection: We went on to investigate the ability of G1-DAPMA and G2-DAPMA to transfect HEK293 cells using a standard luciferase assay, and the data were normalised against branched poly(ethyleneimine) (bPEI, 20k). As observed previously for G1-SPM and G2-SPM, these dendrons, at least in unmodified form, were fairly ineffective in transfection assays (Figure 3).[20] Similar to G1-SPM, den-

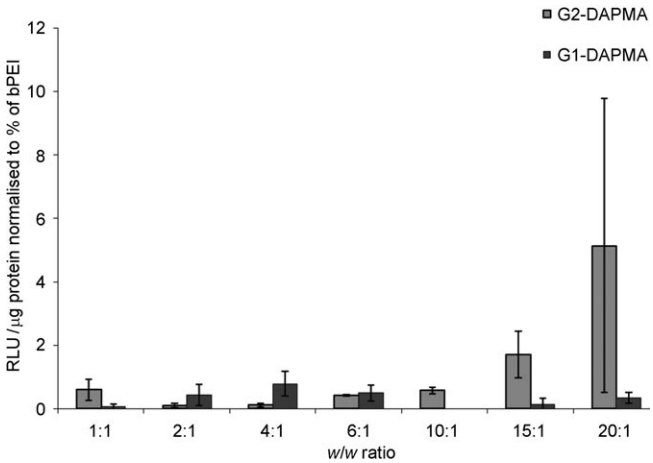

Figure 3. Transfection data for G1-DAPMA and G2-DAPMA for HEK293 cells by using a standard luciferase assay. For G1-DAPMA it was necessary to add chloroquine (100 μM) to observe transfection. Data for G2-DAPMA are chloroquine-free.

dron G1-DAPMA required the addition of chloroquine for effective transfection to be observed, indicative of problems with endosomal escape. However, like G2-SPM, G2-DAPMA was a moderate transfection agent even in the absence of chloroquine. At low loadings, G2-DAPMA gave similar levels of transfection to G2-SPM even though it has fewer amine groups and is a significantly weaker DNA binder (G2-SPM achieved a maximum transfection level of 4% compared with a standard bPEI control; data previously published).[20] Furthermore, G2-DAPMA exhibited the best transfection of all dendrons at relatively high loadings (20:1, *w*/*w*). Presumably high N:P ratios are needed because the DNA binding is weak and sufficient dendron is required to condense the plasmid and protect it in the extracellular environment.

Dendron toxicity: We also monitored the toxicity of the dendrons using a Cell Titer-Blue cell viability assay. Interestingly, both G1-DAPMA and G2-DAPMA were significantly less toxic than bPEI (Figure 4). Indeed, both of these dendrons showed effectively no toxicity up to relatively high concentrations of approximately 40 $\mu g\,mL^{-1}$. This is in sharp contrast to G2-SPM, which exhibited significant toxicity at concentrations above 20 $\mu g\,mL^{-1}$ (data previously published).[20] The relatively lower toxicity of G2-DAPMA perhaps helps explain why it was still an active transfection agent at relatively high loadings, whereas under such conditions G2-SPM is too toxic to effectively transfect cells. It is worth noting that at low loadings, both G1-DAPMA and G2-DAPMA cause significant cell proliferation; this was not observed for G1-SPM or G2-SPM, and the reasons for this are unclear.

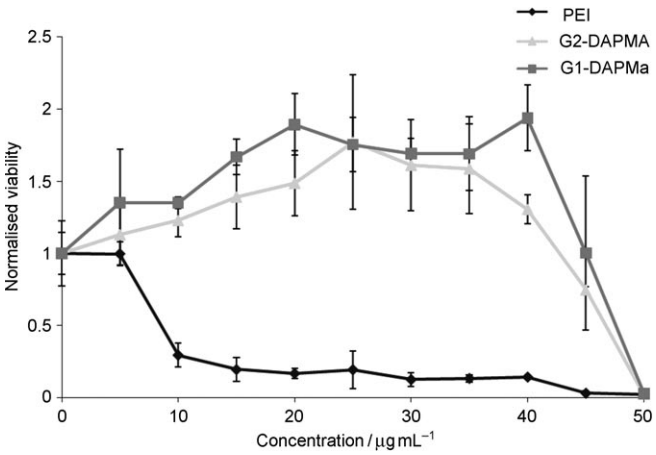

Figure 4. Toxicity data for G1-DAPMA and G2-DAPMA compared with bPEI.

Summary of experimental data: In combination, these results lead us to believe that even though DAPMA surface groups appear to be significantly less effective than SPM in terms of absolute affinity for DNA, these dendrons have potential for further synthetic optimisation as low-toxicity gene delivery agents. This observation is similar to those made for the modification of dendritic structures with arginine units;[13] that is, this modification reduces the affinity of the dendrimers for DNA due to the more charge-diffuse nature of the guaninidium group compared with a simple amine, but lowers toxicity and enhances the observed gene delivery profiles. It is also worth noting that although the absolute levels of transfection for our structures are low, we have previously demonstrated with our SPM-surfaced dendrons that the incorporation of hydrophobic units at the dendron focal point can dramatically enhance gene delivery.[20b] We therefore conclude from these experimental studies that further synthetic modification of the DAPMA-derived dendrons could be worthwhile.

Modelling Study

Molecular dynamics methodology: Given the potential of these dendrons and the interesting experimental DNA binding effects, we decided to model the effect of surface group modification on DNA binding using molecular dynamics (MD) methods in AMBER 9.[25] To achieve this, we employed a 21 base pair B-DNA double strand containing a mixture of bases (Figure 5). This choice relied on a compromise between accuracy and computational feasibility, and was the method previously used for a full modelling study of compounds G1-SPM and G2-SPM.[18] For the purposes of modelling, we assumed that in each dendron structure, all amine groups were protonated. The pK_a values of an isolated spermidine unit are 10.90, 9.71 and 8.25.[26] Spermidine, with three protonatable amines, separated by three- and four-carbon spacers is a good analogue for the surface bound spermine groups, and is, as a consequence of the pK_a values largely protonated at pH 7. Of course, the act of locating multiple spermidine-like amines on the periphery of a dendritic scaffold will modify the pK_a values making full

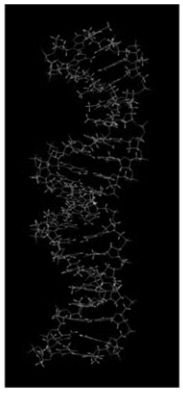

Antisense: 5'-TCG AAG TAC TCA GAG TAA GTT-3'
Sense: 3'-AGC TTC ATG AGT CTC ATT CAA-5'

Figure 5. Structure of the double helical DNA used for modelling in this study.

protonation more difficult, however, the dendritic scaffold is relatively flexible, and a preliminary pH titration indicated that the majority (>90%) of the amines remain protonated at physiological pH, even for G2-SPM.[27] The force-field parameters for these residue types were obtained by using the AM1 semiempirical calculation methods available within the *antechamber* module of AMBER 9. We constructed dendron models for G1-SPM, G2-SPM (previously reported),[18] G1-DAPMA, G2-DAPMA, G1-DAP and G2-DAP (modelled but not synthesised; see above). Each of these models was simulated in a TIP3P water box,[28] with a single DNA double helix and a single dendron unit; binding affinities (ΔG_{bind}) were determined by using molecular dynamics methods under biologically relevant salt (150 mM) conditions (see the Supporting Information for full details). The particle mesh Ewald (PME) approach[29] was used to treat long-range electrostatic effects, and bond lengths involving bonds to hydrogen atoms were constrained by using the SHAKE algorithm.[30] The ΔG_{bind} values were calculated by using the molecular mechanics Poisson–Boltzmann surface area (MM-PBSA) method,[31] taking both polar and nonpolar solvation effects into account.[32] Entropic parameters were estimated by using the normal-mode-analysis approach.[33] The free energies of binding, as well as the enthalpic and entropic contributions, are reported in Table 2 as an average across a number of snapshots obtained from the MD trajectories.

Thermodynamic insights into multivalency: Clearly, each of the dendrons has a favourable interaction with the DNA double helix, as indicated by the negative ΔG_{bind} values. It would be anticipated that as the charge of the dendron increases, so would the strength of its interaction with DNA. This is indeed, in general terms, the case; for example, when comparing G2-SPM (+27) with G1-DAP (+3) it is evident that, as expected, G2-SPM is a much more effective binder (>tenfold increase in binding affinity). This is in agreement with the experimental data. However, Table 2 indicates that the relationship between charge and binding affinity is not a straightforward one, for example, dendrons G2-DAP and G1-SPM both have total charges of +9, but G1-SPM has a more favourable ΔG_{bind} value than G2-DAP. This indicates that the ligand structure plays an important role in organising the individual charge–charge interactions.

It is informative to compare the effective binding energy per dendron charge (ΔG_{bind}/charge, Table 2). It is clear that each charge is most effectively used when the surface groups are SPM (i.e., ca. -7.0 kcal mol^{-1} per charge). Those dendrons with simple DAP surface groups are the least effective in terms of DNA binding (only ca. -5.5 kcal mol^{-1} per charge). Importantly, the ΔG_{bind}/charge values are in general agreement with the CE_{50} values reported in Table 1 and the gel electrophoresis studies; that is, G2-SPM is the most effective binder on a per charge basis, G2-DAPMA and G1-SPM have similar, intermediate affinities for DNA, and the other dendrons (G1-DAPMA and G1-DAP) are significantly less effective DNA binders.

The modelling indicates there is an enthalpy–entropy compensation effect (Table 2). The binding is enthalpically favourable due to electrostatic attraction, but entropically unfavourable due to loss of degrees of freedom. However, closer inspection of the data makes it clear that enthalpy and entropy vary with charge in very different ways. In general terms (with the exception of G1-DAP) each charge contributes approximately -12.0 kcal mol^{-1} to the value of ΔH_{bind}. This is a consequence of the enthalpy of binding largely reflecting the simple electrostatics of interaction between the dendron and the DNA, therefore, the more highly charged the cationic dendron, the stronger the enthalpic interaction with anionic DNA. In contrast to the enthalpies, the entropic values are much less predictable in the way they vary with charge. For example, G2-DAP and G1-SPM both have the same charge (+9) and similar ΔH_{bind} values: (-109.9 kcal mol^{-1} vs. -106.3 kcal mol^{-1}) but the binding of G2-DAP to DNA is entropically much more disfavoured than the binding of G1-SPM ($-T\Delta S_{bind}=+60.2$ kcal mol^{-1} vs. $+45.9$ kcal mol^{-1}). This indicates that more degrees of freedom are lost when G2-DAP binds DNA. It is this entropic difference that leads to the difference in ΔG_{bind} values, with G1-SPM predicted to be a much more effective DNA binder than G2-DAP. Evidently, the binding of the higher generation G2 system, which only has terminal monoamine ligands (G2-DAP), to DNA is not as efficient on entropic grounds as binding a lower generation G1 system with multiple amines on each branch of the dendron (G1-SPM). This provides a key insight into multivalency, although both systems contain nine amines, they are differently arranged. It is clearly better to have the individual amines grouped together into three spermine units, than spread onto the termini of nine separate flexible branches. Anchoring the nine separate branches of a G2 dendron to DNA, although enthalpically equivalent to binding three spermine units in terms of charge–charge interactions, is clearly entropically more challenging due to the required

Table 2. Thermodynamic parameters determined by molecular dynamics methods for the binding of dendrons to DNA. Analysis was performed by using 150 mM aqueous NaCl as solvent medium. All data (apart from charge) are in kcal mol^{-1}.

Dendron	Charge	ΔH_{bind}	$-T\Delta S_{bind}$	ΔG_{bind}	ΔH_{bind}/charge	$-T\Delta S_{bind}$/charge	ΔG_{bind}/charge
G1-DAP	+3	-49.9 ± 5.3	$+33.2\pm12.1$	-16.7	-16.6 ± 1.8	$+11.1\pm4.0$	-5.6
G2-DAP	+9	-109.9 ± 13.5	$+60.2\pm13.8$	-49.6	-12.2 ± 1.5	$+6.7\pm1.5$	-5.5
G1-DAPMA	+6	-68.9 ± 7.0	$+35.1\pm9.2$	-33.8	-11.5 ± 1.2	$+5.9\pm1.5$	-5.6
G2-DAPMA	+18	-227.3 ± 9.5	$+101.0\pm14.8$	-126.3	-12.6 ± 0.5	$+5.6\pm0.8$	-7.0
G1-SPM	+9	-106.3 ± 12.3	$+45.9\pm17.0$	-60.4	-11.8 ± 1.4	$+5.1\pm1.9$	-6.7
G2-SPM	+27	-310.2 ± 11.5	$+114.0\pm14.4$	-196.2	-11.5 ± 0.4	$+4.2\pm0.5$	-7.3

"immobilisation" of the much larger dendritic structure. The importance of entropic factors in driving multivalency effects is often discussed,[2] but this modelling demonstrates an important example in which entropic factors discriminate between multivalent binding effects in two enthalpically equivalent but structurally different dendrons.

In order to probe the binding in more detail, and to better understand the origin of these enthalpic and entropic effects on multivalency, we went on to consider the dendrons as assemblies of residues. Each dendron was considered to be composed of three different kinds of residue (Figure 6). We assigned CEN (yellow) as the benzyl carbamate protecting group at the focal point of the dendron, REP (blue) as the repetitive unit of the Newkome-type dendron (amide–ether repeat unit, Figure 1) and SPM, DAPMA or DAP as the surface amine groups (coloured by atom, Figure 6) in each of the different dendron systems. This decomposition of molecular mechanics energies allowed us to gain an insight into the interaction between each individual residue and the DNA double helix, and hence fully understand the origins of binding.

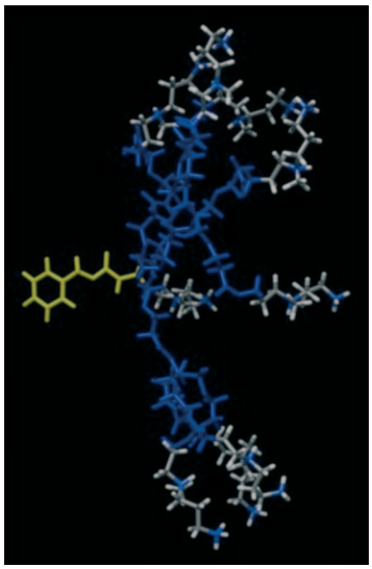

Figure 6. Depiction of G2-DAPMA indicating the three different types of structural residue: CEN (yellow), REP (blue) and SPM (coloured by atom: C in silver, N in blue and H atoms in white).

In Table 3, we report the energetic contributions of each residue within the dendron structure. These can be defined in terms of Equation (1), that is, they represent the difference between the energy of the dendron–DNA complex ($E_{complex}$) and the sum of the energies of dendron and DNA taken separately ($E_{dendron}+E_{DNA}$). Negative energy values indicate attractive forces and the thermodynamic tendency to form a complex:

$$E = E_{complex} - (E_{dendron} + E_{DNA}) \quad (1)$$

Gas-phase energies (E_{gas}) for each residue are composed of electrostatic and van der Waals interaction contributions (E_{ele} and E_{vdw}, respectively) according to Equation (2):

$$E_{gas} = E_{ele} + E_{vdw} \quad (2)$$

The in-vacuum gas-phase energy for each residue (E_{gas}) is then corrected for solvent effects by using the mm pbsa.pl script of AMBER 9 with the generalized Born solvation method (the Poisson–Boltzmann method is not supported in residue-based energy decomposition) to obtain the total energy E_{tot}.[34]

Table 3 presents the contribution of the amine surface groups SPM, DAPMA and DAP to the binding energy for each of the G1 dendrons. This allows direct comparison in binding enthalpy between the different systems. The contributions of the CEN and REP units of the dendron to the binding energy were found to be minimal, and are therefore not presented in Table 3 for clarity. The amine groups are primarily responsible for interacting with the DNA double helix, and as is clear from Table 3, the interaction is wholly electrostatic in nature, with no significant van der Waals contribution. As expected, G1-SPM has the highest affinity

Table 3. Interaction energies determined for individual residues within the G1 dendron structure interacting with DNA. Energies represent the difference between the complex and the two individual components; negative values represent favourable interactions. The total in-vacuum energy E_{gas}, composed of van der Waals E_{vdw} and electrostatic E_{ele} energies is corrected for solvation giving E_{tot}. All energies are reported in kcal mol^{-1}.

Dendron	Residue[e]	Number	E_{vdw}[a]	E_{ele}[b]	E_{gas}[c]	Mean E_{gas} ±SD	E_{tot}[d]	Mean E_{tot} ±SD
G1-DAP	DAP	1	0.2	−351.3	−351.1	−342.2±17.0	−6.6	−6.2±0.7
	DAP	2	−0.2	−356.9	−357.1		−6.9	
	DAP	3	0.1	−318.6	−318.5		−5.2	
	sum of surface amines		0.1	−1026.8	−1026.7		−18.7	
G1-DAPMA	DAPMA	1	0.0	−548.9	−548.9	−635.7±62.5	−7.1	−10.2±2.8
	DAPMA	2	−1.4	−692.4	−693.7		−13.9	
	DAPMA	3	−0.5	−664.0	−664.5		−9.6	
	sum of surface amines		−1.9	−1905.3	−1907.2		−30.6	
G1-SPM	SPM	1	−0.5	−840.8	−841.3	−977.3±127.5	−11.8	−18.5±4.9
	SPM	2	−2.1	−1145.9	−1147.9		−23.1	
	SPM	3	−2.4	−940.3	−942.8		−20.7	
	sum of surface amines		−4.9	−2927.0	−2931.9		−55.7	

[a] E_{vdw} represents the van der Waals interaction energy. [b] E_{ele} represents the electrostatic interaction energy. [c] E_{gas} represents the combination of E_{vdw} and E_{ele} to yield the overall in vacuo nonbond energy. [d] E_{tot} represents the total energy after correction for solvation.

for DNA, G1-DAPMA the next highest and G1-DAP the lowest; this is in agreement with the experimental data. Interestingly, the overall gas-phase interaction energy between G1-DAP (charge = 3) and DNA is approximately 33% of the interaction between G1-SPM (charge = 9) and DNA. The overall gas-phase interaction energy between G1-DAPMA (charge = 6) and DNA is approximately 66% of the interaction between G1-SPM (charge = 9) and DNA. These observations are in agreement with the experimental data and also with the modelling, which indicated that the enthalpic term was basically proportional to the number of charged residues in the dendron.

It is interesting to note the variance in gas-phase interaction energy between the different surface amines. For G1-DAP, the lowest energy is -318.5 kcal mol^{-1}, whilst the highest is -357.1 kcal mol^{-1}, with the standard deviation being about 5.0% of the mean. This indicates that each of the three surface amine groups binds with similar affinity to the DNA double helix. For G1-DAPMA, the standard variation in E_{gas} between the three surface diamine ligands is 9.8% of the mean, whilst for G1-SPM, the standard deviation in E_{gas} between the three surface triamine ligands is as high as 13.0% of the mean, with SPM2 contributing considerably more to the binding than SPM1. Therefore, although the average gas-phase affinity is proportional to the number of charges, not every charge is contributing equally, particularly in the cases in which the surface amine groups are either diamines or triamines. This indicates that for G1-SPM in particular, it is preferable to optimise the interaction of one of the surface polyamine ligands with DNA, even if this compromises somewhat the binding affinity of the other two ligands. This is not the case for G1-DAP, which attempts to optimise the interaction of all three individual point surface charges with DNA. It is clear that in order to optimise all three surface groups simultaneously, G1-DAP will suffer from a much larger relative entropic cost of binding, as the overall dendron structure will lose many degrees of freedom. This observation is in agreement with the data in Table 2, which demonstrated that the entropic cost per interaction ($T\Delta S_{bind}$/charge) for G1-DAP binding to DNA was $+11.1$ kcal mol^{-1}, whilst for G1-SPM it was only $+5.1$ kcal mol^{-1}. These arguments also hold when considering the E_{tot} values, which are corrected for solvation.

Table 4 presents the same kind of analysis applied to the second generation (G2) dendrons. Once again, in agreement with the experimental data, G2-SPM has the highest affinity for DNA, G2-DAPMA is intermediate and G2-DAP has the lowest affinity. However, in this case, the interaction energies are not proportional to dendron charge. Although the E_{gas} of G2-DAP binding to DNA is approximately one third

Table 4. Interaction energies determined for individual residues within the G2 dendron structure interacting with DNA. Energies represent the difference between the complex and the two individual components; negative values represent favourable interactions. All energies are reported in kcal mol^{-1}.

Dendron	Residue[e]	Number	E_{vdw}[a]	E_{ele}[b]	E_{gas}[c]	Mean E_{gas} ±SD	E_{tot}[d]	Mean E_{tot} ±SD
G2-DAP	DAP	14	0.0	−333.2	−333.3	−343.7±39.5	−6.3	−5.1±1.4
	DAP	15	−2.0	−388.2	−390.3		−6.2	
	DAP	16	−0.3	−350.0	−350.3		−7.3	
	DAP	17	−0.3	−334.5	−334.8		−5.6	
	DAP	18	−1.4	−363.4	−364.7		−3.8	
	DAP	19	−1.6	−390.3	−391.9		−3.1	
	DAP	20	−0.2	−305.7	−305.9		−4.0	
	DAP	21	0.0	−259.5	−259.5		−3.5	
	DAP	22	−0.5	−361.7	−362.2		−6.3	
	sum of surface amines		−6.2	−3086.6	3092.7		−46.0	
G2-DAPMA	DAPMA	14	−0.8	−673.8	−674.6	−734.8±95.3	−11.9	−16.9±5.1
	DAPMA	15	−5.6	−805.5	−811.1		−17.6	
	DAPMA	16	−2.7	−877.1	−879.8		−19.0	
	DAPMA	17	−4.2	−841.3	−845.5		−26.4	
	DAPMA	18	−0.6	−705.1	−705.6		−19.2	
	DAPMA	19	−2.6	−763.2	−765.8		−16.3	
	DAPMA	20	−1.4	−653.0	−653.0		−15.2	
	DAPMA	21	−0.1	−561.1	−561.1		−7.0	
	DAPMA	22	−0.9	−716.6	−716.6		−19.9	
	sum of surface amines		−18.9	−6596.7	−6615.6		−152.4	
G2-SPM	SPM	14	−2.1	−979.2	−981.3	−1007.0±151.2	−18.3	−21.3±8.5
	SPM	15	−3.9	−1141.8	−1145.7		−29.4	
	SPM	16	−2.1	−1193.1	−1195.2		−28.9	
	SPM	17	−4.9	−1199.0	−1203.9		−36.1	
	SPM	18	−5.1	−1029.7	−1034.9		−23.6	
	SPM	19	−0.2	−786.2	−786.4		−9.5	
	SPM	20	−1.0	−953.1	−954.1		−18.1	
	SPM	21	−0.1	−763.3	−763.5		−9.7	
	SPM	22	−3.4	−994.3	−997.7		−18.4	
	sum of surface amines		−22.8	−9039.8	−9062.6		−191.9	

[a] E_{vdw} represents the van der Waals interaction energy. [b] E_{ele} represents the electrostatic interaction energy. [c] E_{gas} represents the combination of E_{vdw} and E_{ele} to yield the overall in vacuum nonbond energy. [d] E_{tot} represents the total energy after correction for solvation.

of the binding of G2-SPM, the E_{gas} of G2-DAPMA is significantly larger than the expected 66.6% of G2-SPM (actually 73.0%). This implies that on a per charge basis, G2-DAPMA appears to bind more strongly to DNA than might be predicted/expected. This is even more marked when considering the E_{tot} values (corrected for solvation). For G2-DAP the E_{tot} value is only approximately 24.0% of G2-SPM (i.e., less than expected) whereas for G2-DAPMA it is 79.4% (much more than expected).

Once again, it is interesting to note that for the multivalent surface amines SPM and DAPMA, the interactions between different surface ligands and the DNA are more varied in energy. For G2-DAP the standard deviation in E_{gas} represents 11.5% of the mean, whilst for G2-DAPMA and G2-SPM this figure rises to 13.0 and 15.0%, respectively. The same argument applies for the solvated E_{tot} values, for which the standard deviation rises from 27.5% of the mean for G2-DAP to 30.1 and 39.9% for G2-DAPMA and G2-SPM, respectively. Solvation increases the standard deviation, as it amplifies the differences in DNA binding between different surface ligands on the same dendron because solvent molecules compete for interactions with the surface ligands that are not bound to DNA.

As observed for G1-DAP, G2-DAP attempts to optimise the interaction of as many of the surface point charges as possible with DNA; clearly this will have a significant entropic cost across the whole dendritic structure ($-T\Delta S_{bind}$/charge = +6.7 kcal mol^{-1}, Table 2). There is a greater range of binding energies for the surface ligands of G2-DAP than G1-DAP because it is not actually possible to completely optimise the binding of nine simple surface monoamines to the DNA double helix (also reflected in a lower $-T\Delta S_{bind}$/charge value for G2-DAP than G1-DAP). The inability to organise all of the charge–charge interactions becomes even more marked for G2-DAPMA and G2-SPM; these dendrons clearly only optimise the interaction of selected surface ligands with DNA, the other ligands binding less effectively. However, this selective optimisation will have a lower entropic cost per interaction; indeed for G2-SPM $-T\Delta S_{bind}$/charge is as low as +4.2 kcal mol^{-1} (Table 2) because not all of the dendritic structure requires such careful organisation. This entropic difference helps explain why the dendrons with polyvalent surface amines (SPM and DAPMA) are experimentally so much more effective than those with individual surface amine groups (DAP). This entropically-amplified difference between dendrons is much larger than what would be expected purely from the calculation of charge–charge interactions between the dendrons and DNA.

Structural insights: In order to understand why the binding between G2-DAPMA and DNA appeared to be anomalously large in enthalpic terms (73.0% of G2-SPM in terms of E_{gas} and 79.4% terms of E_{tot}, when charge–charge interactions alone would have led us to expect 66.6%) we performed a structural study of the dendron–DNA binding process. Figure 7 reports the dynamic RMSD (root mean square deviation, defined by Equation (3)) versus simulation time for all G2+DNA complexes, the G2 dendron considered individually within the complex, and the DNA molecule within the complex.

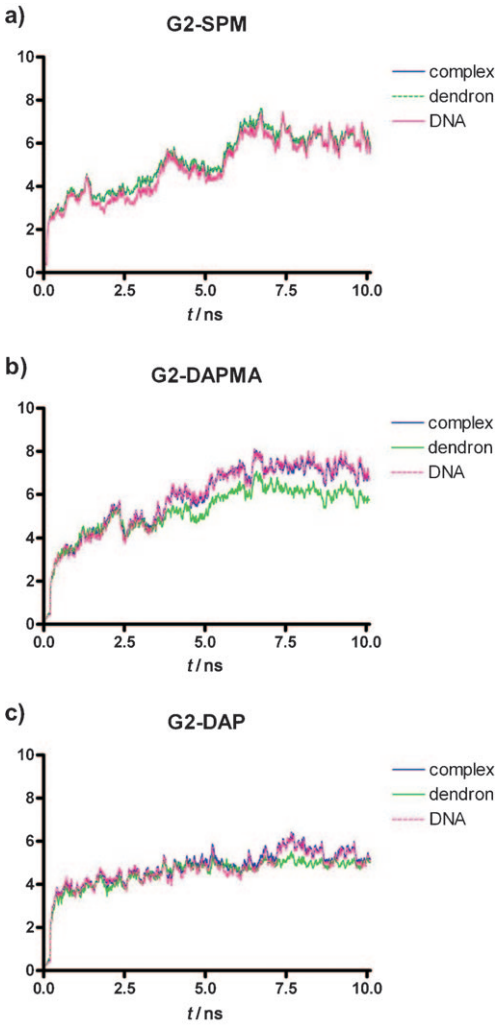

Figure 7. Root mean square deviation (RMSD) of heavy atoms belonging to G2+DNA complexes (blue), G2 dendron (green) and DNA (pink) reported for: a) G2-SPM, b) G2-DAPMA, and c) G2-DAP systems as a function of time (ns) and $\rho(r)$. RMSD represents the movements (Å) of heavy atoms from their starting positions. A horizontal tendency means that the system reached an equilibrium (i.e., the system is uniformly vibrating).

In Equation (3) δ is the distance between N pairs of equivalent heavy atoms (in this study C, N, O and P atoms belonging to dendron and DNA molecules only, water excluded). This allows us to represent the way in which each heavy atom of the structure moves from the starting position in the simulation. As the value reaches a plateau, it represents the system having evolved to constant vibration around an equilibrium position (i.e., the system has reached equilibrium in the simulation).

$$\mathrm{RMSD} = \sqrt{\frac{1}{N}\sum_{i=1}^{i=N}\delta_i^2} \qquad (3)$$

It is interesting to compare the behaviour of the curves for the complex and the two individual components (i.e., dendron and DNA) and to consider their superposition (Figure 7). For G2-SPM the curves are perfectly superimposed (Figure 7a), indicating that the complex is uniform, with the vibration of atoms in the two individual components being equivalent to the vibration of the overall complex. However, for G2-DAPMA there is a significant difference between the curves (Figure 7b) with the dendron having significantly lower RMSD values than the DNA or the overall complex. This is due to the dendron conformation (the different RMSD values mean that the position of the dendron is shifted from the starting position by about 6 Å, whereas the DNA atoms shift by about 7 Å for DNA). The DAPMA-functionalised dendrons appear to have a degree of structural rigidity—a consequence of the different structure of the DAPMA ligand compared with SPM (we suggest this might be a consequence of the presence of the methyl group on the tertiary amine of DAPMA; see later for further discussion). However, it is worth noting that, after reaching a convergence in RMSD, the curves proceed in parallel, meaning that dendron and DNA atoms, after reaching an equilibrium position, do vibrate uniformly as a stable complex. For G2-DAP the situation is rather different; there is reasonable superposition between the curves, but at points, the RMSD for the dendron diverges from the other curves (Figure 7c). This is indicative of a weaker binding, with the monoamine end groups of the DAP structure being less attractive to DNA than the diamines and triamines of DAPMA and SPM, and hence the vibrations of dendron and DNA differ from one another over the time-course of the simulation.

Table 5 reports the radius of gyrations (R_g) for the G2+DNA complexes, the G2 dendrons, the DNA molecule, and also the surface ligands (each considered within the simulated complex). This radius of gyration, as defined by Equation (4) represents the average distance between each atom in the structure considered and the centre of mass of the dendron.

Table 5. Radius of gyration (R_g, as defined by Equation (4)), which represents the distance of atoms from the centre of mass of the dendron. The data considered the whole dendron, the surface amine ligands of the dendron, and the DNA (all within the complex) as well as the overall complex between dendron and DNA.

Dendron	R_g (dendron)/Å	R_g (surface ligands)/Å	R_g (DNA)/Å	R_g (complex)/Å
G2-DAP	10.2	12.8	20.6	19.5
G2-DAPMA	11.8	13.8	19.2	18.2
G2-SPM	15.4	18.1	21.7	20.4

$$R_g^2 = \frac{1}{N}\sum_{k=1}^{N}(r_k - r_{mean})^2 \quad (4)$$

As is evident from Table 5, the dendron R_g for G2-SPM (15.4 Å) is larger than that for G2-DAPMA (11.8 Å) or G2-DAP (10.2 Å) as expected based on the relative sizes of these dendrons. Considering only the surface ligands of the dendron leads to larger radii of gyration than the overall dendron structure, as the surface ligands are the furthest points, most distant from the centre of mass. However, it is noteworthy that the difference between surface ligands and dendron is smallest for G2-DAPMA (only 2.0 Å) not, as may have been expected G2-DAP (2.6 Å), which actually has smaller ligand groups. This indicates that the surface ligands of G2-DAPMA are not fully extended when they interact with the DNA. Furthermore, the dimensions of the overall complex are actually the smallest when G2-DAPMA is used, and the DNA is significantly smaller (2.5 Å) in this case than when the surface ligand is SPM. This indicates that the G2-DAPMA dendron deforms the DNA in order to achieve its interactions, whereas for the binding of G2-SPM and G2-DAP the DNA remains more extended. There has been recent literature interest in the different abilities of oligoamines to modify the conformational preferences of DNA, and in some cases it has been suggested that unnatural amines are more likely to encourage conformational change.[35]

This DNA deformation/bending can be observed visually in the molecular mechanics structural models (Figure 8). We suggest that by bending DNA in this way, G2-DAPMA is able to achieve larger interaction energies than would have been predicted on a simple "per charge" basis (helping explain the stronger than expected energetic data for G2-DAPMA in Table 4). It also explains why the entropy of DNA binding is more disfavoured for G2-DAPMA than G2-SPM, as deforming DNA in this way will lose significant degrees of freedom.

In a final analysis to probe why the DAPMA surface ligands appear to have this kind of effect, we considered the detailed radial distribution functions (RDFs) rather than just the simple averaged radii of gyration values presented in Table 5. Figure 9a, b, and c represent the overall RDFs. Since RDF, indicating the presence of atoms in space (i.e., as a function of the distance from the centre of mass of the dendron) is calculated at each frame of simulation, it has a clear dynamic meaning. Large peaks in these graphs mean not only high density of atoms in a certain zone, but also high localisation, and thus low ability of these atoms to move. The contact point between dendron and DNA corresponds with the peak maximum, close to the centre of mass, meaning that at this point degrees of freedom are lost because of the dendron–DNA interactions. Figure 9d, e, and f represent the distributions of phosphorus (on DNA) and nitrogen (on the surface amines). The contact peak between anionic phosphate and cationic protonated amine is clearly visible as the peak maximum close to the centre of mass in each case. Interestingly, however, for G2-DAP the peak for the protonated amine (Figure 9f, solid line) is significantly smaller than for G2-DAPMA or G2-SPM (Figure 9d and e, solid lines). This lower peak indicates that the terminal

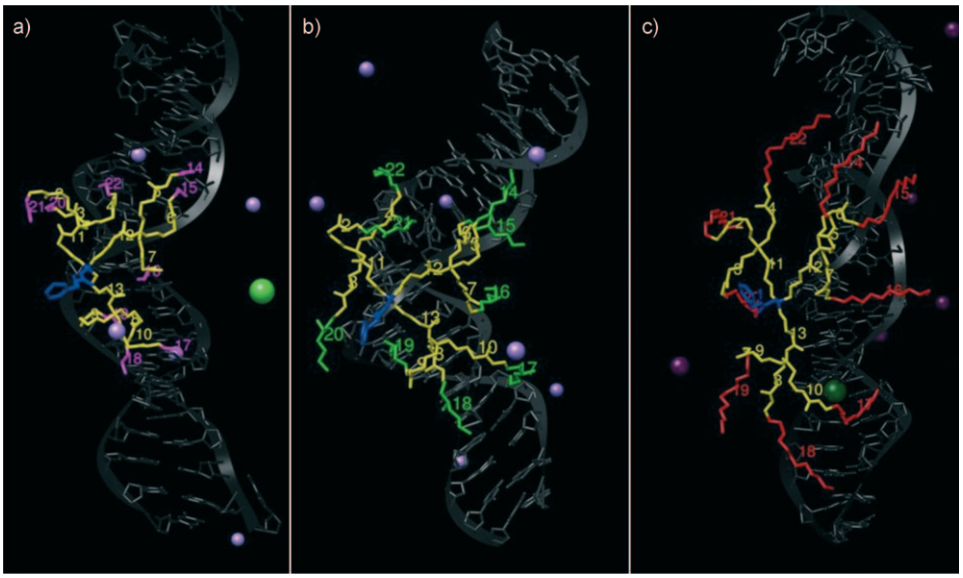

Figure 8. Snapshots of molecular dynamics simulation of G2 dendrons binding to double helical DNA: a) G2-DAP, b) G2-DAPMA, and c) G2-SPM. Within the dendron CEN is shown in blue, REP in yellow and the amine ligands are shown in magenta (DAP), green (DAPMA) and red (SPM). The DNA is portrayed as a dark grey shadow, water molecules are omitted for clarity, and only those counterions in close proximity to the complexes are shown.

amines of G2-DAP are more likely to be oscillating around the P atoms of DNA; this is consistent with the relatively lower binding of this system, and in agreement with our arguments above about the significant entropic cost (per charge) of binding G2-DAP to the DNA double helix. For G2-SPM and G2-DAPMA on the other hand, the multivalent nature of each individual amine ligand helps counteract the entropic cost of immobilisation and lowers the mobility of the main electrostatic contact point between dendron and DNA.

Figure 10a and b represent the radial distribution function for the ligating nitrogen atoms of the surface amines in G2-SPM and G2-DAPMA. This

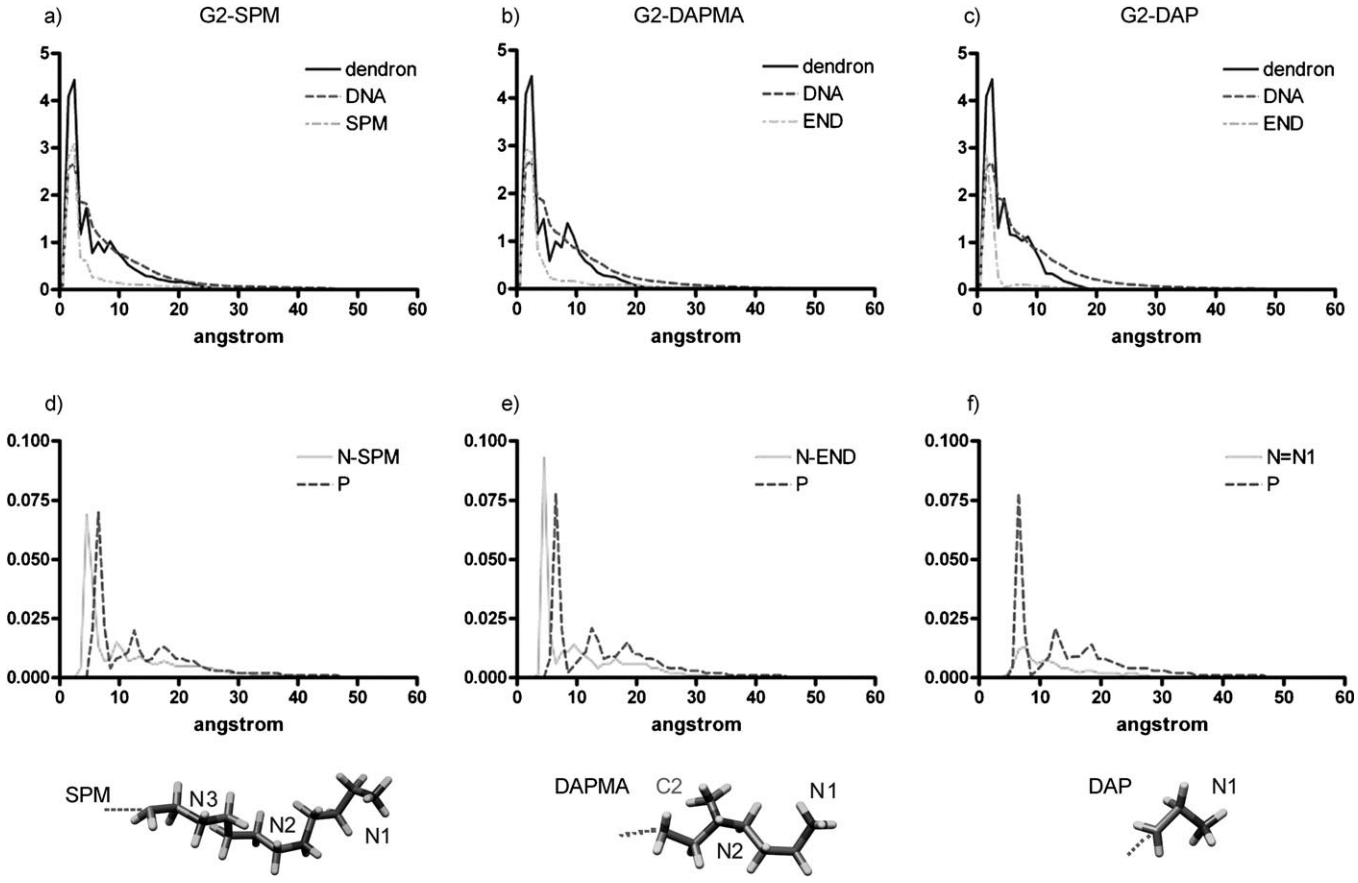

Figure 9. Radial distribution functions (RDF) of dendron (——), DNA (-----) and surface ligands (–•–•) are reported for: a) G2-SPM, b) G2-DAPMA, and c) G2-DAP. RDF of N atoms of surface ligands (——) and of P atoms of DNA (-----) are reported for: d) G2-SPM, e) G2-DAPMA, and f) G2-DAP. Surface SPM, DAPMA and DAP ligands are illustrated in the bottom of the panel and shaded by atoms (N dark grey, C grey and H white). The most crucial atoms of these surface ligands are labelled with decreasing index going toward the surface.

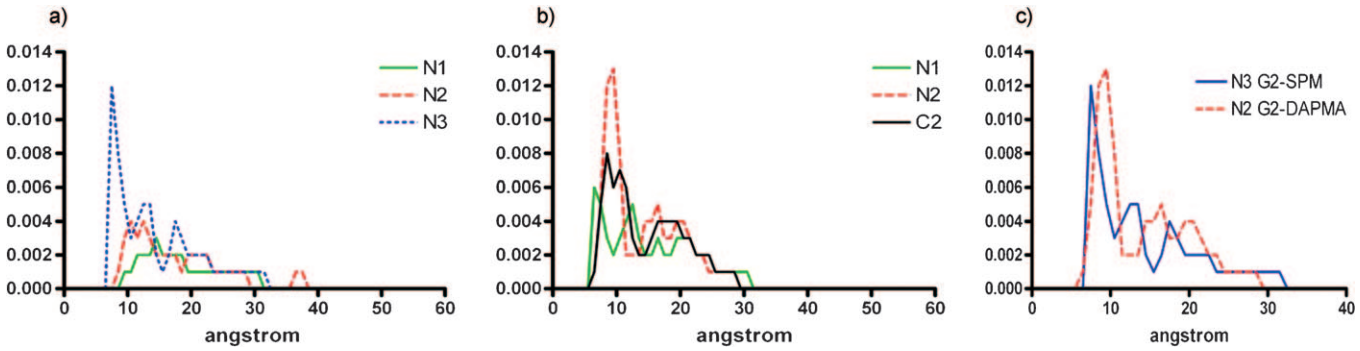

Figure 10. RDF of selected atoms of surface ligands reported for: a) G2-SPM, and b) G2-DAPM. RDF for N1 is represented in green, for N2 in red and for N3 and C2 in blue and black, respectively. Superposition of RDF of most internal amines of SPM (N3, blue) and DAPMA (N2, red) represents the difference in peaks c).

analysis allows a structural decomposition of the role of each individual protonated amine within the complex with DNA. Figure 10b also presents the radial distribution function for the methyl group (identified by C2 atom) attached to the tertiary amine (N2 position) of DAPMA. For G2-SPM it is evident that N3 forms the most stable interaction with DNA (i.e., the highest peak corresponding to the lowest mobility). This is the amine closest to the dendron scaffold. The amines N2 and, to an even greater extent N1, then form more mobile interactions with the DNA (i.e., smaller peaks), which are further away from the centre of mass. For G2-DAPMA, the primary interaction is formed by N2 (again closest to the dendritic scaffold). This peak is larger than that observed for N3 of G2-SPM (Figure 10c), which indicates a lower mobility of this amine in G2-DAPMA than in G2-SPM. Notably, the attached methyl group appears coincident with the amine, indicating it is located in the same region of space. We argue that this group hinders the mobility of the N2 group once bound to the DNA. Terminal atom N1 also forms interactions with DNA, but these can be either closer to the centre of mass than the primary interaction between N2 and DNA (surprising) or further away (as expected and as was observed for G2-SPM). This indicates the important/primary role played by the sterically hindered N2 in the binding process, with the remainder of the DAPMA group then forming the best remaining interaction available, which might require either ligand back-folding or ligand extension. Ligand back-folding can be seen for some of the DAPMA ligands in Figure 8b (e.g., 16 and 17) but is not observed for any of the spermine ligands in Figure 8c. We propose that the steric hindrance of the N2 group of DAPMA and the strong preference for its coordination to the DNA double helix provides the stronger than expected enthalpic interaction with DNA, causes ligand back-folding, and ultimately leads to the structural deformation of DNA discussed above. SPM ligands on the other hand, are more optimised for binding in the minor groove, and therefore ligand back-folding and DNA deformation are not observed to any major extent.

Summary and Conclusion

By synthesising a family of dendrons with varied surface amine ligands we have gained a unique insight into DNA binding, gene delivery and multivalency effects. It was shown that the dendrons with spermine (SPM) surface groups are the most effective DNA binders. The dendrons with DAP and DAPMA surface groups are less effective at DNA binding. However, the DAPMA-functionalised dendrons were more effective systems for gene delivery with low toxicity, performing as well as, if not better than the SPM-functionalised dendrons (although the gene delivery profiles were still relatively modest).

In order to provide deeper insight into the experimental data, we performed a molecular dynamics simulation of the interactions between the dendrons and DNA. The results of these simulations demonstrated that in general terms, the enthalpic contribution to binding was proportional to the degree of surface charge, but dendrons with DAP and DAPMA surface amines had significant entropic costs of binding, which limited their total binding affinity. In the case of DAP, this is a consequence of the fact that the entire dendron structure had to be organised in order for all of the monoamine ligand charges to make effective contact with DNA. In contrast, for SPM, each surface ligand is already a multivalent triamine, therefore, each individual charge has a much lower entropic cost of binding. For DAPMA, we observed that binding of the hindered amine to the DNA was enthalpically stronger than expected and also caused ligand back-folding, which led to significant geometric distortion of the DNA double helix. This weakened the overall binding from what may have been expected solely on the grounds of the enthalpic charge–charge interactions. We suggest that this geometric distortion could help explain the experimentally observed enhanced gene delivery—DNA compaction is an important step in transfection.

Overall, this study demonstrates how we can begin to develop structure–activity relationships for multivalent dendritic ligands using a combined experimental and theoretical approach. The paper supports other work showing that gene delivery potential does not necessarily correlate with bind-

ing strength. Importantly, our approach provides key insights into the thermodynamics of multivalency for structurally related dendritic ligands, in particular the subtle ways in which enthalpy and entropy control the binding process.

Acknowledgements

We thank Nathan P. Gabrielson and Prof. Daniel W. Pack for assistance with the gene transfection studies, which were carried out in the Department of Chemical Engineering at University of Illinois at Urbana–Champaign. The generous financial support to the DRUDE Initiative, project "Nanovectors for drug delivery in oncology: a combined modelling/experimental study" performed under the project framework "Computational Life Science promoted by USI" and sponsored by DECS Canton Ticino to A.D. and S.P., is gratefully acknowledged. D.K.S. also acknowledges EPSRC (C534395/1) in funding this research. All researchers acknowledge the support of COST action TD0802, "Dendrimers in Biomedical Applications", in enabling this collaborative program of research.

[1] a) M. Mammen, S.-K. Choi, G. M. Whitesides, *Angew. Chem.* **1998**, *110*, 2908–2953; *Angew. Chem. Int. Ed.* **1998**, *37*, 2754–2794; b) A. Mulder, J. Huskens, D. N. Reinhoudt, *Org. Biomol. Chem.* **2004**, *2*, 3409–3424; c) J. D. Badjic, A. Nelson, S. J. Cantrill, W. B. Turnbull, J. F. Stoddart, *Acc. Chem. Res.* **2005**, *38*, 723–732.

[2] See for example: a) J. Huskens, A. Mulder, T. Auletta, C. A. Nijhuis, M. J. W. Ludden, D. N. Reinhoudt, *J. Am. Chem. Soc.* **2004**, *126*, 6784–6797; b) E. L. Doyle, C. A. Hunter, H. C. Philips, S. J. Webb, N. H. Williams, *J. Am. Chem. Soc.* **2003**, *125*, 4593–4599; c) C. W. Lim, B. J. Ravoo, D. N. Reinhoudt, *Chem. Commun.* **2005**, 5627–5629; d) R. J. Mart, K. P. Liem, X. Wang, S. J. Webb, *J. Am. Chem. Soc.* **2006**, *128*, 14462–14463; e) C. W. Lim, O. Crespo-Biel, M. C. A. Stuart, D. N. Reinhoudt, J. Huskens, B. J. Ravoo, *Proc. Natl. Acad. Sci. USA* **2007**, *104*, 6986–6991.

[3] a) F. Vögtle, G. Richardt, N. Werner, A. J. Rackstraw, *Dendrimer Chemistry—Concepts, Syntheses, Properties, Applications*, Wiley-VCH, Weinheim, **2009**; b) G. R. Newkome, C. N. Moorefield, *Handbook of Dendrimers: Synthesis Nanoscience and Applications*, Wiley-VCH, Weinheim, **2009**; c) D. A. Tomalia, *Prog. Polym. Sci.* **2005**, *30*, 294–324; d) U. Boas, J. B. Christensen, P. M. H. Heegaard, *Dendrimers in Medicine and Biotechnology*, Royal Society of Chemistry, Cambridge, **2006**; e) B. Klajnert, M. Bryszewska, *Dendrimers in Medicine*, Nova Science UK, **2007**; f) I. J. Majoros, J. R. Baker, *Dendrimer-Based Nanomedicine*, Pan Stanford, Singapore, **2008**.

[4] a) C. Dufes, I. F. Uchegbu, A. G. Schatzlein, *Adv. Drug Delivery Rev.* **2005**, *57*, 2177–2202; b) M. Guillot-Nieckowski, S. Eisler, F. Diederich, *New J. Chem.* **2007**, *31*, 1111–1127; c) H. S. Parekh, *Curr. Pharm. Des.* **2007**, *13*, 2837–2850; d) D. K. Smith, *Curr. Top. Med. Chem.* **2008**, *8*, 1187–1203; e) A.-M. Caminade, C. O. Turrin, J.-P. Majoral, *Chem. Eur. J.* **2008**, *14*, 7422–7432.

[5] a) S. Y. Wong, J. M. Pelet, D. Putnam, *Prog. Polym. Sci.* **2007**, *32*, 799–837; b) M. J. Tiera, F. M. Winnik, J. C. Fernandes, *Curr. Gene Ther.* **2006**, *6*, 59–71.

[6] a) J. Haensler, F. C. Szoka, *Bioconjugate Chem.* **1993**, *4*, 372–379; b) J. F. Kukowska-Latallo, A. U. Bielinska, J. Johnson, R. Spindler, D. A. Tomalia, J. R. Baker, *Proc. Natl. Acad. Sci. USA* **1996**, *93*, 4897–4902; c) A. Bielinska, J. F. Kukowska-Latallo, J. Johnson, D. A. Tomalia, J. R. Baker, *Nucleic Acids Res.* **1996**, *24*, 2176–2182; d) M. X. Tang, C. T. Redemann, F. C. Szoka, *Bioconjugate Chem.* **1996**, *7*, 703–714.

[7] Selected references include: a) M. X. Tang, F. C. Szoka, *Gene Ther.* **1997**, *4*, 823–832; b) A. U. Bielinska, C. L. Chen, J. Johnson, J. R. Baker, *Bioconjugate Chem.* **1999**, *10*, 843–850; c) N. Malik, R. Wiwattanapatapee, R. Klopsch, K. Lorenz, H. Frey, J. W. Weener, E. W. Meijer, W. Paulus, R. Duncan, *J. Controlled Release* **2000**, *65*, 133–148; d) D. Luo, K. Haverstick, N. Belcheva, E. Han, W. M. Saltzman, *Macromolecules* **2002**, *35*, 3456–3462; e) H. G. Abdelhady, S. Allen, M. C. Davies, C. J. Roberts, S. J. B. Tendler, P. M. Williams, *Nucleic Acids Res.* **2003**, *31*, 4001–4005; f) J. Zhou, J. Wu, N. Hafdi, J.-P. Behr, P. Erbacher, L. Peng, *Chem. Commun.* **2006**, 2362–2364; g) T. Takahashi, C. Kojima, A. Harada, K. Kono, *Bioconjugate Chem.* **2007**, *18*, 1349–1354.

[8] a) W. Chen, N. J. Turro, D. A. Tomalia, *Langmuir* **2000**, *16*, 15–19; b) S. V. Lyulin, A. A. Darinskii, A. V. Lyulin, *Macromolecules* **2005**, *38*, 3990–3998; c) P. K. Maiti, B. Bagchi, *Nano Lett.* **2006**, *6*, 2478–2485.

[9] Selected references include: a) M. Ohsaki, T. Okuda, A. Wada, T. Hirayama, T. Niidome, H. Aoyagi, *Bioconjugate Chem.* **2002**, *13*, 510–517; b) I. Toth, T. Sakthivel, A. F. Wilderspin, H. Bayele, M. O'Donnell, D. J. Perry, K. J. Pasi, C. A. Lee, A. T. Florence, *STP Pharm. Sci.* **1999**, *9*, 93–99; c) J. S. Choi, D. K. Joo, C. H. Kim, K. Kim, J.-S. Park, *J. Am. Chem. Soc.* **2000**, *122*, 474–480; d) A. V. Kiselev, P. L. Il′ina, A. A. Egorova, A. N. Baranov, I. A. Guryanov, N. V. Bayanova, I. I. Tarasenko, E. A. Lesina, G. P. Vlasov, V. S. Baranov, *Russ. J. Gen. Chem.* **2007**, *43*, 593–600.

[10] See for example: a) B. H. Zinselmeyer, S. P. Mackay, A. G. Schatzlein, I. F. Uchegbu, *Pharm. Res.* **2002**, *19*, 960–967; b) T.-i. Kim, J.-u. Baek, C. Z. Bai, J.-S. Park, *Biomaterials* **2007**, *28*, 2061–2067.

[11] a) D. Joester, M. Losson, R. Pugin, H. Heinzelmann, E. Walter, H. P. Merkle, F. Diederich, *Angew. Chem.* **2003**, *115*, 1524–1528; *Angew. Chem. Int. Ed.* **2003**, *42*, 1486–1490; b) C. Loup, M.-A. Zanta, A.-M. Caminade, J.-P. Majoral, B. Meunier, *Chem. Eur. J.* **1999**, *5*, 3644–3650; c) A. V. Maksimenko, V. Mandrouguine, M. B. Gottikh, J.-R. Bertrand, J.-P. Majoral, C. Malvy, *J. Gene Med.* **2005**, *7*, 61–71; d) M. Guillot, S. Eisler, K. Weller, H. P. Merkle, J.-L. Gallani, F. Diederich, *Org. Biomol. Chem.* **2006**, *4*, 766–769.

[12] N. D. Sonawane, F. C. Szoka, A. S. Verkman, *J. Biol. Chem.* **2003**, *278*, 44826–44831.

[13] a) J. S. Choi, K. Nam, J.-Y. Park, J.-B. Kim, J.-K. Lee, J.-S. Park, *J. Controlled Release* **2004**, *99*, 445–456; b) J.-B. Kim, J.-S. Choi, K. Nam, M. Lee, J.-S. Park, J.-K. Lee, *J. Controlled Release* **2006**, *114*, 110–117; c) T. Okuda, A. Sugiyama, T. Niidome, H. Aoyagi, *Biomaterials* **2004**, *25*, 537–544; d) H. Y. Nam, K. Nam, H. J. Hahn, B. H. Kim, H. J. Lim, H. J. Kim, J. S. Choi, J.-S. Park, *Biomaterials* **2009**, *30*, 665–673.

[14] M. A. Kostiainen, J. G. Hardy, D. K. Smith, *Angew. Chem.* **2005**, *117*, 2612–2615; *Angew. Chem. Int. Ed.* **2005**, *44*, 2556–2559.

[15] a) S. S. Cohen, *A Guide to Polyamines*, Oxford University Press, Oxford, **1998**; b) K. Igarashi, K. Kashiwagi, *Biochem. Biophys. Res. Commun.* **2000**, *271*, 559–564.

[16] a) D. Bancroft, I. D. Williams, A. Rich, M. Egli, *Biochemistry* **1994**, *33*, 1073–1086; b) V. A. Bloomfield, *Biopolymers* **1997**, *44*, 269–282; c) I. Rouzina, V. A. Bloomfield, *Biophys. J.* **1998**, *74*, 3152–3164; d) M. Saminathan, T. Anthony, A. Shirahata, L. H. Sigal, T. Thomas, T. J. Thomas, *Biochemistry* **1999**, *38*, 3821–3830; e) L. D. Williams, *Annu. Rev. Biophys. Biomol. Struct.* **2000**, *29*, 497–521; f) H. Deng, V. A. Bloomfield, J. M. Benevides, G. J. Thomas, *Nucleic Acids Res.* **2000**, *28*, 3379–3385; g) V. Vijayanathan, T. Thomas, A. Shirahata, T. J. Thomas, *Biochemistry* **2001**, *40*, 13644–13651; h) Y. Burak, G. Ariel, D. Andelman, *Biophys. J.* **2003**, *85*, 2100–2110; i) L. D′Agostino, M. di Pietro, A. Di Luccia, *FEBS J.* **2005**, *272*, 3777–3787; j) D. Pastre, O. Pietrement, F. Landousy, L. Hamon, I. Sorel, M. O. David, E. Delain, A. Zozime, E. Le Cam, *Eur. Biophys. J.* **2006**, *35*, 214–223.

[17] a) N. Korolev, A. P. Lyubartsev, A. Laaksonen, L. Nordenskiöld, *Biophys. J.* **2002**, *82*, 2860–2875; b) N. Korolev, A. P. Lyubartsev, A. Laaksonen, L. Nordenskiöld, *Nucleic Acids Res.* **2003**, *31*, 5971–5981; c) N. Korolev, A. P. Lyubartsev, A. Laaksonen, L. Nordenskiöld, *Eur. Biophys. J.* **2004**, *33*, 671–682; d) Y. Burak, G. Ariel, D. Andelman, *Curr. Opin. Colloid, Interface Sci.* **2004**, *12*, 53–58; e) E. Allahyarov, H. Löwen, G. Gompper, *Phys. Rev. E* **2003**, *68*, 061903.

[18] G. M. Pavan, A. Danani, S. Pricl, D. K. Smith, *J. Am. Chem. Soc.* **2009**, *131*, 9686–9694.

[19] a) M. A. Kostiainen, G. R. Szilvay, D. K. Smith, M. B. Linder, O. Ikkala, *Angew. Chem.* **2006**, *118*, 3618–3622; *Angew. Chem. Int. Ed.* **2006**, *45*, 3538–3542; b) M. A. Kostiainen, G. R. Szilvay, J. Lehtinen, D. K. Smith, M. B. Linder, A. Urtti, O. Ikkala, *ACS Nano* **2007**, *1*, 103–113.
[20] a) J. G. Hardy, M. A. Kostiainen, D. K. Smith, N. P. Gabrielson, D. W. Pack, *Bioconjugate Chem.* **2006**, *17*, 172–178; b) S. P. Jones, N. P. Gabrielson, D. W. Pack, D. K. Smith, *Chem. Commun.* **2008**, 4700–4702.
[21] a) M. A. Kostiainen, D. K. Smith, O. Ikkala *Angew. Chem.* **2007**, *119, 7744–7748; Angew. Chem. Int. Ed.* **2007**, 46, 7600–7604; *Angew. Chem. Int. Ed.* **2007**, *46*, 7600–7604; b) D. J. Welsh, S. P. Jones, D. K. Smith, *Angew. Chem.* **2009**, *121*, 4107–4111; *Angew. Chem. Int. Ed.* **2009**, *48*, 4047–4051; c) M. A. Kostiainen, H. Rosilo, *Chem. Eur. J.* **2009**, *15*, 5656–5660.
[22] a) G. R. Newkome, X. Lin, *Macromolecules* **1991**, *24*, 1443–1444; b) C. M. Cardona, R. E. Gawley, C. Gawley, *J. Org. Chem.* **2002**, *67*, 1411–1413.
[23] M. Pittelkow, R. Lewinsky, J. B. Christensen, *Synthesis* **2002**, 2195–2202.
[24] a) B. F. Cain, B. C. Baguley, W. A. Denny, *J. Med. Chem.* **1978**, *21*, 658–668; b) H. Gershon, R. Ghirlando, S. B. Guttman, A. Minsky, *Biochemistry* **1993**, *32*, 7143–7151; c) R. Zadmard, T. Schrader, *Angew. Chem.* **2006**, *118*, 2769–2772; *Angew. Chem. Int. Ed.* **2006**, *45*, 2703–2706.
[25] D. A. Case, T. A. Darden, T. E. Cheatham et al. *AMBER 9*, University of California, San Francisco, CA, USA, **2006**.
[26] M. M. Kimberly, J. H. Goldstein, *Anal. Chem.* **1981**, *53*, 789–793.
[27] J. G. Hardy, Ph.D. Thesis, University of York, **2006**.
[28] W. L. Jorgensen, J. Chandrasekhar, J. D. Madura, R. W. Impey, M. L. Klein, *J. Chem. Phys.* **1983**, *79*, 926–935.
[29] T. Darden, D. York, L. Pedersen, *J. Chem. Phys.* **1993**, *98*, 10089–10092.
[30] a) J.-P. Ryckaert, G. Ciccotti, H. J. C. Berendsen, *J. Comput. Phys.* **1977**, *23*, 327–341; b) V. Kräutler, W. F. van Gunsteren, P. H. Hunenberger, *J. Comput. Chem.* **2001**, *22*, 501–508.
[31] J. Srinivasan, T. E. Cheatham, P. Cieplak, P. A. Kollman, D. A. Case, *J. Am. Chem. Soc.* **1998**, *120*, 9401–9409.
[32] a) B. Jayaram, D. Sprous, D. L. Beveridge, *J. Phys. Chem. A* **1998**, *102*, 9571–9576; b) D. Sitkoff, K. A. Sharp, B. Honig, *J. Phys. Chem.* **1994**, *98*, 1978–1988; c) M. F. Sanner, A. J. Olson, J. C. Spehner, *Biopolymers* **1996**, *38*, 305–320.
[33] I. Andricioaei, M. Karplus, *J. Chem. Phys.* **2001**, *115*, 6289–6292.
[34] P. A. Kollman, I. Massova, C. Reyes, B. Kuhn, S. Huo, L. Chong, M. Lee, T. Lee, Y. Duan, W. Wang, O. Donini, P. Cieplak, J. Srinivasan, D. A. Case, T. E. Cheatham, *Acc. Chem. Res.* **2000**, *33*, 889–897.
[35] a) N. Narayana, N. Shamala, K. N. Ganesh, M. A. Viswamitra, *Biochemistry* **2006**, *45*, 1200–1211; b) C. N. N'soukpoe-Kossi, A. A. Ouameur, T. Thomas, A. Shirahata, T. J. Thomas, H. A. Tajmir-Riahi, *Biomacromolecules* **2008**, *9*, 2712–2718.

Received: September 15, 2009
Revised: January 27, 2010
Published online: March 16, 2010

